

SBR SWITCHING BY FUZZY PATTERN RECOGNITION

S. Marsili-Libelli

*Department of Systems and Computers
University of Florence
Via S. Marta, 3 – 50139 Florence, ITALY
Email: marsili@dsi.unifi.it*

Abstract: The Sequencing Batch Reactor (SBR) is a widely used process for biological removal of nutrients (nitrogen and phosphorus) from wastewater. It is normally operated on a fixed switching schedule, resulting in an inefficient process operation. This paper proposes a switching strategy based on an adaptive fuzzy inferential engine. In this way the duration of each phase is limited to the time strictly necessary for the actual loading conditions. Experimental results show that the treatment cycle can be significantly shortened, with the results that more wastewater can be treated. *Copyright © 2005 IFAC*

Keywords: Pattern recognition, fuzzy inference, artificial intelligence, water pollution, process control.

1. INTRODUCTION

The Sequencing Batch Reactor (SBR) process is increasingly used for biological nutrient removal from wastewater (Kern-Jespersen and Henze, 1993; Wilderer et al., 2001). At the same time, more stringent water quality standards are being introduced, which cannot be met unless wastewater treatment processes are upgraded (Oles and Wilderer, 1991). Therefore efficient control strategies are needed, in order to adapt the process operation to the ever changing requirements resulting from the varying wastewater composition. Normally SBR are operated in a cyclic manner involving five phases: loading, anoxic-anaerobic treatment, aerobic treatment, sedimentation, effluent extraction. Each phase has a fixed duration regardless of the process requirements and this may result in a highly inefficient operation in terms of the time allocated to each phase. Moreover, wrong

timing may result in a serious process degradation, especially when phosphorus removal is involved.

The aim of this paper is to illustrate the application of artificial intelligence tools to the detection of critical process transitions and drive the switching accordingly. In this way the duration of each phase will last exactly as required. Moreover, the detection should be based only on simple indirect measurements, given the difficulty of directly observing the process variables.

After recalling the key points of the SBR operation, the artificial intelligence tools will be introduced and finally the application will be presented and its performance assessed.

1.1. Indirect process indicators

The alternate operation of SBR hinges on the feast/famine metabolism of Phosphorus Accumulating Organisms (PAO) to obtain the biological removal of both phosphorus and nitrogen

(Smolders et al., 1995; Murnleitner et al., 1997). Basically, denitrification occurs in anoxic conditions, whereas phosphorus is removed whenever the organism are driven through a transition from anaerobic to aerobic conditions. Normally SBR are switched according to a fixed time-pattern, allocating 30 minutes to loading, 120 minutes to the anaerobic/anoxic phase, 150 minutes to the aerobic phase and the last 60 minutes to the combined settling and extraction phase, for a total of 6 hours. This rigid scheme may be very far from optimal because the two central phases (anaerobic/anoxic and aerobic) are largely load-dependent and their duration should be tuned to the actual process requirements, hence the need to adjust switching according to the state of the process. If all the relevant process quantities (i.e. ammonium-N, Nitrate-N and Phosphate-P) were available in real-time, switching could be performed according to the following simple rules:

- The anaerobic/anoxic phase ends when both the nitrate-N has been denitrified and all the available organic carbon is used in the process. At this time the aeration should be switched on;
- The aerobic phase ends when all the phosphate-P is taken up by the PAO or all the ammonium-N is converted into nitrate-N, whichever takes longer. At this time the aeration should be switched off.

There is, unfortunately, a formidable obstacle preventing the implementation of this simple scheme, represented by the complexity of measuring the above quantities in real-time, which is neither simple nor economical. As an alternative, the state of the process can be inferred through easily measurable process variables such as pH, Oxido-Reduction Potential (ORP) and Dissolved Oxygen (DO). The aim of this paper is to use these indirect variables to derive pattern indicators to signal the end of each phase and switch the process accordingly. The existence of significant process patterns can be demonstrated by inspecting the following Figures 1 and 2, representing the typical behaviour during the anaerobic/anoxic and the aerobic phases, obtained with a 2-litre bench-scale pilot plant with synthetic feed operated at the ENEA, Wastewater Division laboratory in Bologna, Italy, and described in Marsili-Libelli et al. (2001) and Spagni et al. (2001).

1.2. Anaerobic/anoxic patterns

During this phase, including the preliminary loading operation, the pH-influencing processes are denitrification and P-release, occurring in this order. The end of former is signalled by a brief pH increase, after which it decreases as a consequence of phosphorus release. The ORP further decreases as the process gets deeper into anaerobic conditions. Eventually when all the available nitrate is denitrified and all phosphorus released, both pH and ORP level off. In Figure 1 this phase ends at time 150 min, because of the fixed timing, but the relevant processes have all ended long before, so

there is a considerable potential for shortening the anaerobic period without impairing process efficiency.

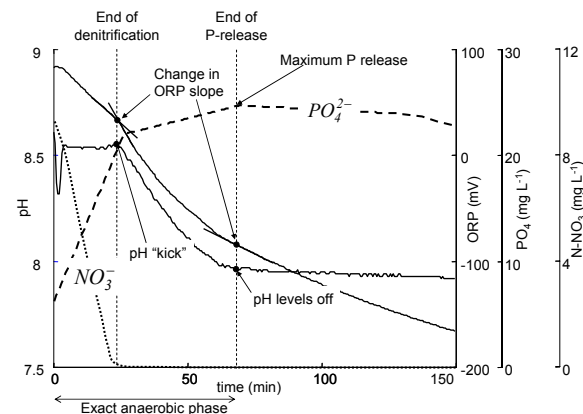


Fig. 1. Process behaviour during the anaerobic - anoxic phase.

In summary, the relevant transitions indicating the end of this phase are the changes in ORP slope and the “kick” and levelling of pH.

1.3. Aerobic patterns

During this phase ammonia is oxidized into nitrate, whereas phosphorus is utilised by the PAO provided that no organic carbon is available. The relevant process variables pH and DO, with the former showing an inflexion at the end of phosphorus uptake and the latter levelling off when all the ammonia has been oxidized, as shown in Figure 2. However, since during the aerobic phase nitrification and P-uptake are concurrent processes, pH may exhibit differing patterns depending on which ends first. This complex behaviour has been examined by Spagni et al. (2001) who observed differing pH patterns as a consequence of the relative duration of two concurrent process: ammonia oxidation and P-uptake, in addition to CO₂ stripping, responsible for a rapid increase of pH at the beginning of the aerobic phase.

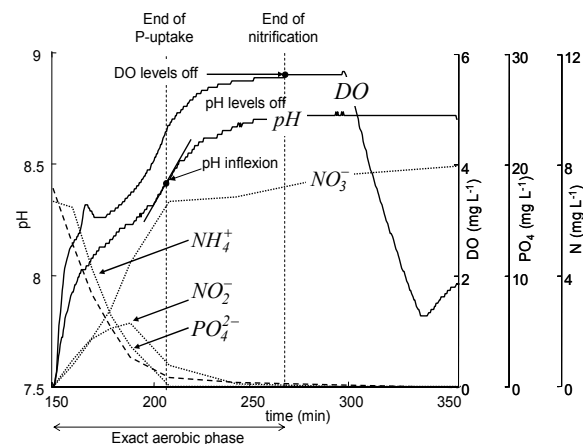


Fig. 2. Process behaviour during the aerobic phase.

Figure 3 shown the two most likely behaviours, depending on whichever process is shorter. In Figure 3.a nitrification ends before P uptake: the end of ammonia oxidation is marked by a change in the slope of pH, but it is difficult to detect the so-called “ammonia valley”.

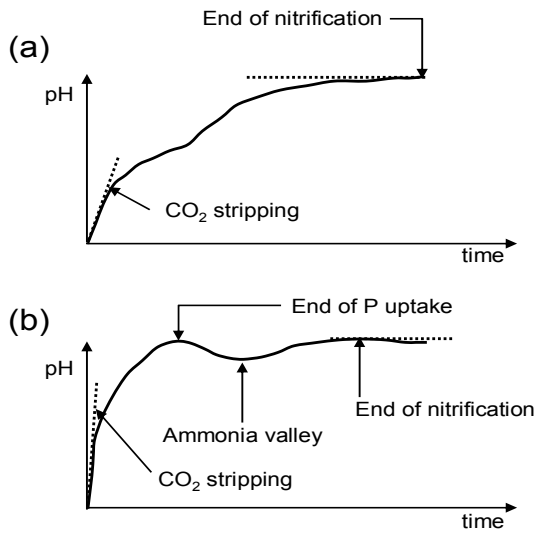


Fig. 3. Possible pH patterns during the aerobic phase.

In Figure 3.b P-uptake ends before nitrification: in this case the “ammonia valley” is very well identified, confirming the effect of P-uptake on pH. In the first part of the aeration phase, pH increase is due to CO₂ stripping and P uptake, when the latter ends pH starts decreasing due to ammonia oxidation. The “aerobic pH apex” can be related to the end of P uptake.

2. PATTERN DETECTION AND FEATURES EXTRACTION

From the behaviours shown in Figures 1 - 3 the relevant patterns in Table 1 are isolated. However, the practical implementation of an inferential engine extracting this information involves several processing steps, from preliminary filtering to numerical differentiation to pattern recognition and feature extraction.

Table 1 Process indicators

Phase	Terminated process	Indicator
Anaerobic anoxic	Denitrification	pH kicks up and then falls; ORP negative slope increases.
	P- release	pH slope levels off.
Aerobic	Nitrification	DO slope levels off.
	P- uptake	pH inflexion point.

The sequence of operations forming the required inferential engine is shown in Figure 4.

2.1. Wavelet processing

From Table 1 it appears that all the relevant patterns are composed of signal derivatives, hence the need to filter the process data and derive then in a numerically robust way. Both steps were carried out with the aid of wavelet processing, using a **db8** basis wavelet (Strang and Nguyen, 1996) in a multilevel decomposition where the second approximation represents a suitable denoised

version of the relevant signals. In this way a sufficiently “clean” signal was recovered and stable derivatives obtained.

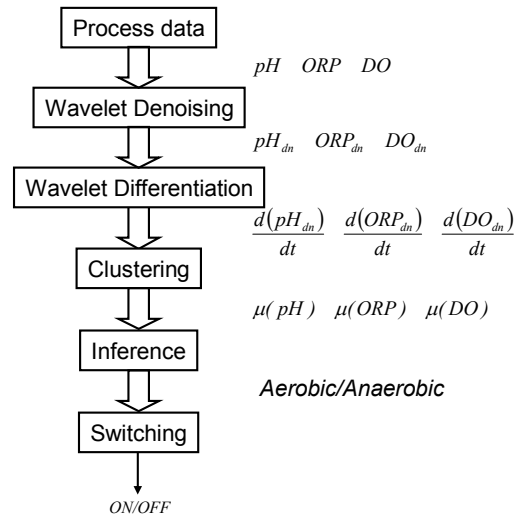


Fig. 4. Processing sequence in the inferential engine.

2.2. Fuzzy clustering

Once the derivative signals have been obtained, they were classified according to the patterns of Table 1. Though a successful neural networks application already exists (Luccarini et al., 2001), a fuzzy approach to pattern recognition (Marsili-Libelli and Müller, 1996) is considered here as an alternative and a Gustafsson-Kessel fuzzy clustering algorithm was selected for its variable metric (Babuska, 1998).

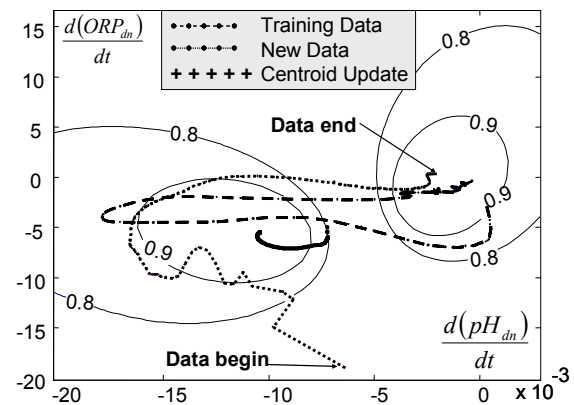


Fig. 5. Adaptive data clustering during the anaerobic/anoxic phase.

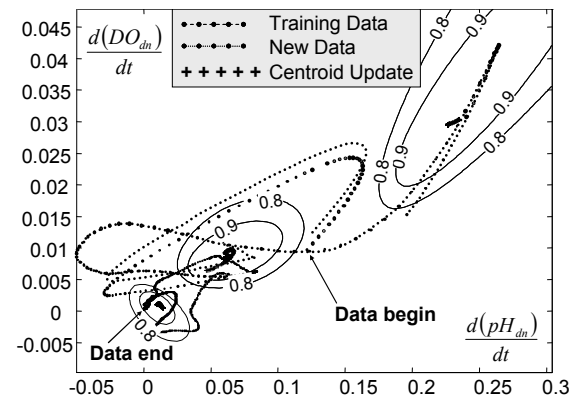


Fig. 6. Adaptive data clustering during the aerobic phase.

The best number of clusters for each phase was determined by minimization of the normalized information entropy H_n (Bezdek, 1981) defined as a function of the membership functions $\mu_{i,k}$

$$H_n = \frac{1}{1 - \frac{c}{N}} \sum_{i=1}^c \sum_{k=1}^N \mu_{i,k} \cdot \log(\mu_{i,k}) \quad (1)$$

Where c is the number of clusters and N the number of data. Applying this definition to the GK clusters of the anaerobic and aerobic data, the graphs of Figure 7 were obtained, indicating that $c_{AN} = 2$ and $c_{AER} = 3$ was the best partition.

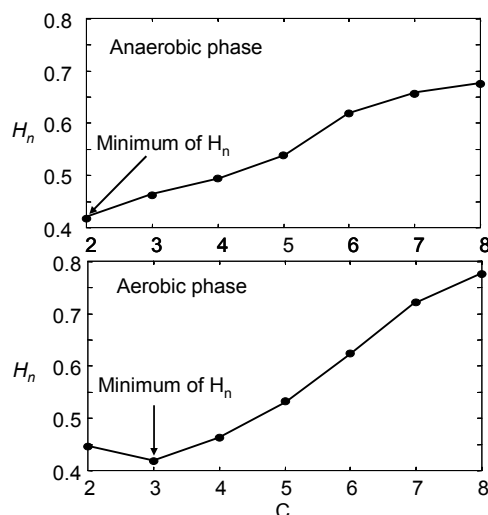


Fig. 7. Normalized partition entropy as a function the number of clusters, used to determine the best partition for both phases.

During operation, the initial clusters resulting from the preliminary training were adapted using again an entropy criterion, thoroughly explained in Marsili-Libelli (1998). Each new data was classified according to the already obtained partition function and the partition matrix U updated with this new membership only if the relative entropy variation

$$\Delta H_n(j) = \frac{H_n(U_j) - H_n(U_{j-1})}{H_n(U_{j-1})} \quad (2)$$

was negative or only slightly positive. In this way the clusters adjust their shape to the changing operational environment.

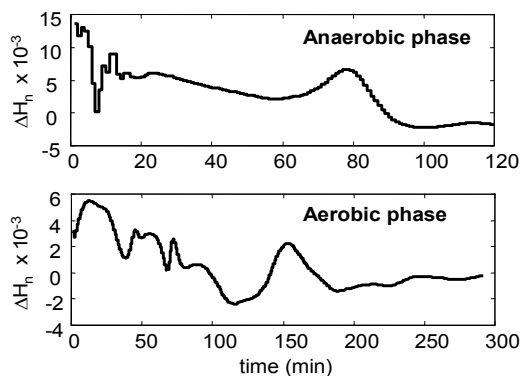


Fig. 8. Entropy variation during adaptive operation.

Figure 8 shows the entropy variations during the adaptive operation, indicating a general tendency towards entropy decrease during operation.

2.3. Inferential engine

According to the cluster structure determined in the previous section, the inference engine has two rules for the former and three rules for the latter situation. The antecedents are AND-ed with a time-duration check, to prevent premature termination of the phase, introducing the time variable with two fuzzy sets $[T_{AN}^1 T_{AN}^2]$ and $[T_{OX}^1 T_{OX}^2]$ for each phase. The complete fuzzy inference mechanism then takes the form of Figure 9.

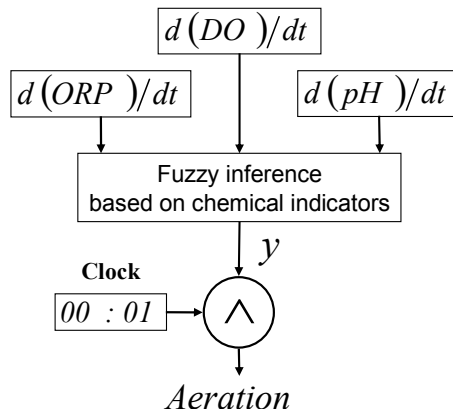


Fig. 9. Inference engine including timing.

The sigmoidal functions for the timing limitation are shown in Figure 10 for either phase. The aerobic phase should last longer to insure consistent ammonia oxidation, whereas the minimum anaerobic duration is related to loading and denitrification.

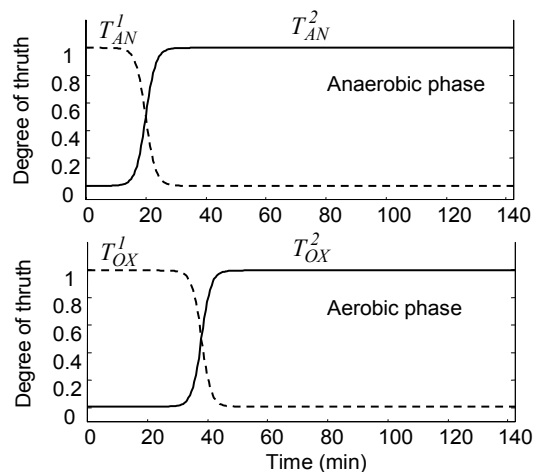


Fig. 10. Fuzzyfication of the phase time variable.

The definition of the consequents is straightforward, assuming that $y = 0$ means that the process in the anaerobic phase and $y = 1$ indicates end of the anaerobic phase. The recognition of the aerobic phase requires three clusters (see Figure 7) and the corresponding output values $y = [0 \ 0.7 \ 1.0]$ define the membership to the aerobic phase. The complete fuzzy inference engine is then described by the following equations:

Anoxic/Anaerobic phase

$$R_{AN}^1 : IF \left[\frac{dpH}{dt}, \frac{dORP}{dt} \right] \in C_1 \text{ AND } t \in T_{AN}^1 \text{ THEN } y_{AN}^1 = 0 \quad (3)$$

$$R_{AN}^2 : IF \left[\frac{dpH}{dt}, \frac{dORP}{dt} \right] \in C_2 \text{ AND } t \in T_{AN}^2 \text{ THEN } y_{AN}^2 = 1$$

$$y_{AN} = \frac{\sum_{i=1}^2 y_{AN}^i \mu_{AN}^i}{\sum_{i=1}^2 \mu_{AN}^i} \quad (4)$$

Aerobic phase

$$R_{OX}^1 : IF \left[\frac{dpH}{dt}, \frac{dDO}{dt} \right] \in C_{OX}^1 \text{ AND } t \in T_{OX}^1 \text{ THEN } y_{OX}^1 = 0 \quad (5)$$

$$R_{OX}^2 : IF \left[\frac{dpH}{dt}, \frac{dDO}{dt} \right] \in C_{OX}^2 \text{ AND } t \in T_{OX}^2 \text{ THEN } y_{OX}^2 = 0.7$$

$$R_{OX}^3 : IF \left[\frac{dpH}{dt}, \frac{dDO}{dt} \right] \in C_{OX}^3 \text{ AND } t \in T_{OX}^3 \text{ THEN } y_{OX}^3 = 1$$

$$y_{OX} = \frac{\sum_{i=1}^3 y_{OX}^i \mu_{OX}^i}{\sum_{i=1}^3 \mu_{OX}^i} \quad (6)$$

The output variable y represents the likelihood of the phase, and will be further “hardened” to produce the required crisp On/Off switching variable. The control output is obtained from either y_{AN} or y_{OX} , whichever is active, via thresholding with an α -cut = 0.95. Figures 11 and 12 show the result of the fuzzy engine operation for either phase. Switching occurs well ahead of the usual fixed timing, indicating that a considerable time saving is possible.

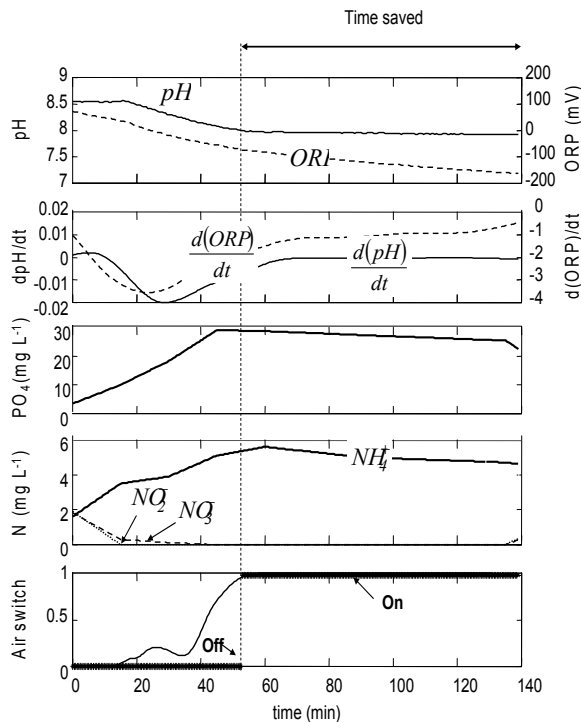


Fig. 11. Fuzzy inference and switching function for the anaerobic/anoxic phase.

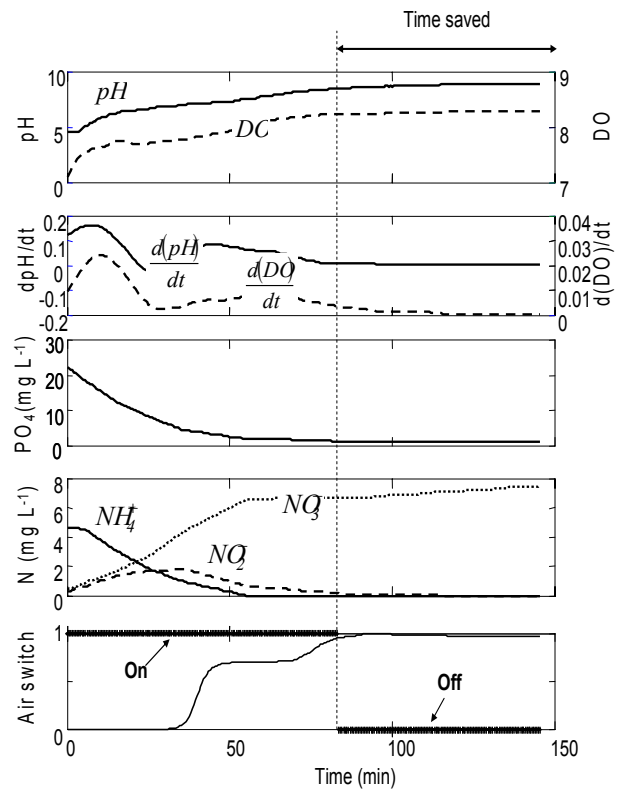


Fig. 12. Fuzzy inference and switching function for the aerobic phase.

2.4. Process implementation

The inferential mechanism just described was first implemented in the Matlab platform (The Mathworks Inc., Natick, USA) and then tested on a 2-litre pilot plant at the ENEA laboratories in Bologna, where the fuzzy algorithm was implemented in real-time using the Labview platform (National Instruments, Austin, USA).

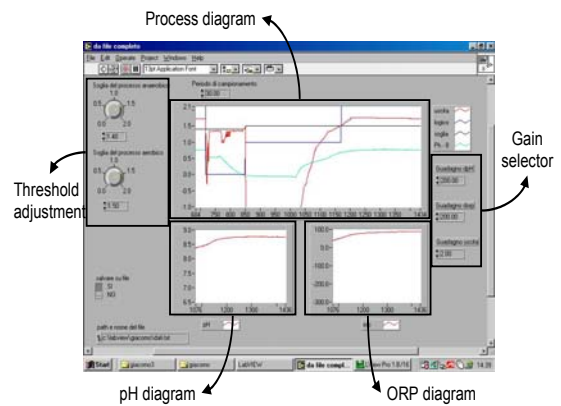


Fig. 13. Front panel of the real-time Labview implementation.

The improvement of this switching control are shown in Figure 14, where the pH and ORP variables are recorded. It can be seen that there is a considerable time saving with respect to the fixed-time arrangement. In fact, this is usually determined with ample margin due to the lack of process measurements.

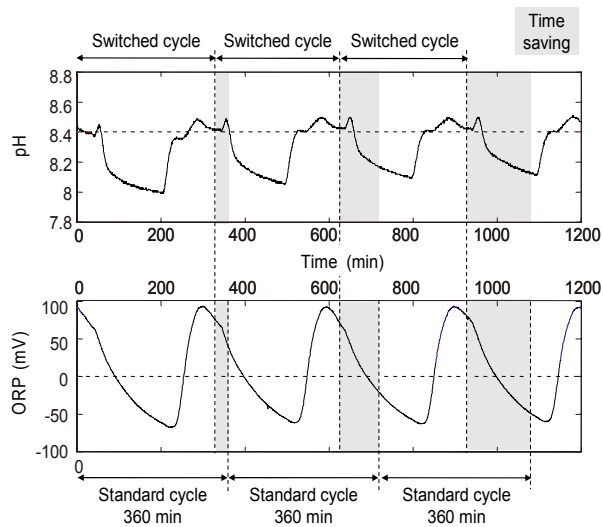


Fig. 14. Time saving obtained with the fuzzy switching strategy.

By contrast, the proposed switching strategy, determining the end of each phase as a result of the inference process, provides a tight switching control. Thus for each cycle two advantages are achieved: the timing is adapted to the current loading conditions and each phase does not last more than needed. In this way a shorter cycle is obtained, with a considerable time saving, which implies that in a given time more cycles can be performed and therefore more wastewater can be treated.

3. CONCLUSION

This paper has presented an inferential engine to control the timing of a Sequencing Batch Reactor (SBR), a process largely used in biological nutrient removal. Normally, this process, which requires a periodic switching between anaerobic and aerobic conditions, is operated on a fixed time-schedule for the lack of process information. The proposed strategy controls timing as the result of an inference process whereby indirect process indicators, represented by pH, ORP and DO, give information about the state of the process through a fuzzy clustering algorithm to decide whether each phase is about to end. This information constitutes the antecedent of a fuzzy reasoning whose output is the switching decision variable. The training and test data were obtained from a pilot plant, on which the switching algorithm was then tested, showing that a significant time saving could be achieved with respect to conventional fixed timing.

REFERENCES

Bezdek, J.C. (1981). *Pattern recognition with fuzzy objective function algorithms*, Plenum Press, New York.

Babuska, R., (1998). *Fuzzy modeling for control*. Kluwer Publ. Co., Amsterdam, 260 pp.

Kern-Jespersen, J.P. and Henze, M. (1993). Biological phosphorus removal from wastewater by aerobic-anoxic sequencing batch reactors. *Wat. Res.* **27**, 617 – 624.

Luccarini, L., Porrà, E., Spagni, A., Ratini, P., Grilli, S., Longhi, S. and Bortone, G. (2001). Soft sensors for control of nitrogen and phosphorus removal from wastewaters by neural networks. *Wat. Sci. Tech.* **45** (4-5): 101 – 107.

Marsili-Libelli S., Müller A. (1996). Adaptive fuzzy pattern recognition in the anaerobic digestion process. *Pattern Recognition Letters*, **17**: 651 – 659.

Marsili-Libelli S. (1998). Adaptive fuzzy monitoring and fault detection. *Int. J. COMADEM*, **1** (3): 31 – 38.

Marsili-Libelli S., Ratini P., Spagni A., Bortone G. (2001). Implementation, study and calibration of a modified ASM2d for the simulation of SBR processes. *Water Sci. Tech.*, **43** (3): 69 – 76.

Murnleitner, E., Kuba, T., van Loosdrecht, M.C.M., Heijnen, J.J. (1997). An integrated metabolic model for the aerobic and denitrifying biological phosphorus removal. *Biotech Bioeng.* **54**: 434 - 450.

Oles, J. and Wilderer, P.A. (1991). Computer aided design of sequencing batch reactors based on the IAWPRC activated sludge model. *Water Sci. Technol.* **23** (4 – 6), 1087 – 1095.

Smolders, G.J.F., van Loosdrecht, M.C.M., Heijnen, J.J. (1995). A metabolic model for the biological phosphorus removal process. *Wat. Sci. Tech.*, **31** (2): 79-93.

Spagni, A., Buday, J., Ratini, P. and Bortone, G. (2001). Experimental considerations on monitoring ORP, pH, conductivity and dissolved oxygen in nitrogen and phosphorus biological removal processes. *Wat. Sci. Tech.* **43** (11): 197 – 204.

Strang, G. and T. Nguyen, *Wavelets and Filter Banks*, Wellesley-Cambridge Press, 1996.

Wilderer, P., Irvine, R.L. and M.C. Goronszy (2001). *Sequencing batch reactors technology*. IWA Scientific and Technical Report n. 10, IWA Publ. London.